Multi-Criteria Analysis of Sensor Reliability for Wearable Human Activity Recognition

Yilin Dong, Jean Dezert, Rigui Zhou, Changming Zhu, Xinde Li, Shuzhi Sam Ge

Multi-Criteria Analysis of Sensor Reliability for Wearable Human Activity Recognition

Yilin Dong, Xinde Li, *Senior Member, IEEE,* Jean Dezert, Rigui Zhou, Changming Zhu and Shuzhi Sam Ge, *Fellow, IEEE*

LIST OF MATHEMATICAL SYMBOLS

$m(\cdot)$	mapping function
Θ	Frame of Discernment
θ	focal element when $m(\theta) > 0$
K	the degree of conflict
$\|\theta\|$	the cardinality of θ
ω	the discounting factor
A	independent sensor
M	number of sensors
$S(\cdot)$	the score function
N	number of criteria
$\mathbf{X}$	original dataset
p	number of attributes
L	number of instances
h_t	input labeled data at time step t
$\sigma(\cdot)$	sigmoid function
C_t, $\tilde{C}_t$	memory states in LSTM
W_{in}, W_f, W_C, W_o	involved weights in LSTM
b_{in}, b_f, b_C, b_o	involved biases in LSTM
$\hat{y}$	outputs of softmax layer in LSTM
n	the number of classes

***Abstract*—In Body Sensor Networks (BSNs), evaluating reliability of sensors is an important research topic which aims to optimize the overall performance of BSNs. Previous studies have often addressed this problem based only on a single criterion. However, it is often unreliable to rely on a single criterion to assess sensors in real situations. Accordingly, in this paper, we propose a novel multi-criteria approach for evaluating sensor reliability in activity recognition problem based on belief function theory. Specifically, in the theoretical part, we first describe the Multi-Criteria Analysis of Sensor Reliability (MCASR) using Belief Function based the Technique for Order Preference by Similarity to Ideal Solution (BF-TOPSIS). And in our proposed MCARS, two criteria are chosen in this work: 1) the conflict between sensor readings and, 2) the imprecision of sensor readings. In the application part, in order to prove the efficiency of MCASR, we propose a novel fused Long-Short Term Memory (LSTM) with MCASR to solve the problem of activity recognition. By using our proposed strategy, the final recognition accuracy has been significantly improved as compared with classical methods.**

***Index Terms*—Sensor Reliability, Belief Function Theory, Multi-Criteria, Activity Recognition, Body Sensor Networks.**

This work was supported in part by the National Natural Science Foundation of China under Grant 61573097; 91748106; 62073072, in part by the Key Laboratory of Integrated Automation of Process Industry under Grant PALN201704, in part by Science and Technology on Information System Engineering Laboratory, No:05201905, 05202003, in part by key projects of key R & D Program of Jiangsu Province under Grant BE2020006, BE2020006-1. (*Corresponding author: Xinde Li.*)

Yilin Dong is with College of Information Engineering, Shanghai Maritime University. Email:yldong@shmtu.edu.cn.

Xinde Li is with Key Laboratory of Measurement and Control of CSE, School of Automation, Southeast University. Email:xindeli@seu.edu.cn.

Jean Dezert is with The French Aerospace Lab, ONERA, DTIS/MSDA, F-91123 Palaiseau, France. Email:jean.dezert@onera.fr.

Rigui Zhou is with College of Information Engineering, Shanghai Maritime University, Shanghai, China. Email:rgzhou@shmtu.edu.cn.

Changming Zhu is with College of Information Engineering, Shanghai Maritime University, Shanghai, China. Email:cmzhu@shmtu.edu.cn.

Shuzhi Sam Ge is with the Social Robotics Laboratory, Department of Electrical and Computer Engineering, Interactive Digital Media Institute, National University of Singapore, Singapore 117576. Email: samge@nus.edu.sg.

I. INTRODUCTION

OVER the past twenty years, Body Sensor Networks (BSNs) [1–7] attract much attention from academia and industry because of the necessity to help more and more elderly or disable people to prevent accidents. Considering that the data in BSNs usually come from multiple sensors, multi-sensor fusion technology has received considerable attention in transforming multi-source inconsistent data into high-quality fusion data [8]. However, the information collected by the sensors in BSNs is usually imperfect in actural environment. Thus, several classical uncertainty theories have been proposed such as probability theory [9], Belief Function theory (BF) [10, 11], fuzzy set theory [12]. Among them, BF theory has been widely used in the field of multi-sensor data fusion with its flexibility to deal with uncertainty [1]. Thus, the topic of this article mainly focus on BF theory. Usually, the actual system often assume that the input data itself is equally reliable in the early stage of fusion process. However, in reality, the performance of the fusion system depends to a large extent on the sensors' own sensing capabilities (for example, stability, accuracy, energy consumption, sensing range, etc.). Therefore, data provided by the involved sensors often does not have the same reliability, and the information to be fused should be modified according to the reliability of its source. In other words, we should strengthen the influence of information provided by more reliable sources, while weakening the influence of information from less reliable sources.

In order to evaluate the reliability of sensors, the proper criterion needs to be chosen judiciously. In fact, research works like [13–16] and [17] present several proposals, that assess the sensors using different single criterion. The representative criteria are Fisher information [13, 15], error covariance [16, 17] and mutual information [18, 19]. But, the use of only a single criterion to evaluate the involved sensors is, however, disputable since this strategy is not enough sufficient to provide the comprehensive assessment. Thus, we herein consider the

multi-criteria decision-making strategy to solve the complex issues where multiple inconsistent sensor measurements have happened. The multi-criteria evaluation method used in this work is the Belief Function based the Technique for Order Preference by Similarity to Ideal Solution (BF-TOPSIS) [20]. Thanks to BF-TOPSIS, the reliability of sensors in BSNs can be easily evaluated using multiple assessment criteria.

The main contributions of this paper are described as follows:

- BF-TOPSIS is used to evaluate sensors more seriously according to multi-criteria. Instead of assessing the involved sensors using only one criteria, we evaluate the sensors in terms of conflicts between sensors and the imprecisions of sensor readings;
- To prove the effectiveness of our new Multi-Criteria Analysis of Sensor Reliability (MCASR), we apply it to solve daily activity recognition problems. In our proposed framework of activity recognition, we first apply the Long-Short Time Memory (LSTM) network to model sequential data and generate the sensor readings. Afterwards, the MCASR strategy is used to assess these sensor readings before combination. Then, the classical discounting combination rule in BF theory is used to combine these sensor readings with the obtained weights;
- In order to evaluate the effectiveness of our proposed activity recognition model, we use the UCI $mHealth$ dataset to test the performance of our proposed model, and focus on the analysis of the impacts of some important parameters.

Section II introduces the basic concepts of BF. Then, the proposed MCASR is illustrated in the third section. Section IV describes the proposed activity recognition system using MCASR in details. The fifth section gives the detailed experimental results on an activity recognition application. Several tests and comparisons are also described. The final section includes a brief conclusion.

II. Basics of BF

In BF theory, mass of belief is often assigned to the subsets in the set of Frame of Discernment (FoD). Generally, the mathematical symbol $m(\cdot)$ represents the mapping function which is defined as follows [21]: for $\theta \subseteq 2^{\Theta}$,

$$m : 2^{\Theta} \to [0,1], \sum_{\theta \subseteq 2^{\Theta}} m(\theta) = 1, \tag{1}$$

$$m(\emptyset) = 0, m(\theta) > 0. \tag{2}$$

In BF theory, m is also called Basic Belief Assignment (BBA) and the set of focal elements of a BBA $m(\cdot)$ is denoted $\mathcal{F}(m)$.

The classical Dempster's rule [21] is often used to combine two independent Sources of Evidence (SoEs), which is denoted as $m_1 \oplus m_2$ and defined as follows: for $\forall \theta \subseteq 2^{\Theta}, \theta \neq \emptyset$,

$$(m_1 \oplus m_2)(\theta) = \frac{1}{1-K} \cdot \sum_{\theta_1,\theta_2 \subseteq 2^{\Theta}, \theta_1 \cap \theta_2 = \theta} m_1(\theta_1) m_2(\theta_2). \tag{3}$$

where K represents the degree of conflict between m_1 and m_2 as:

$$K = \sum_{\theta_1,\theta_2 \subseteq 2^{\Theta}, \theta_1 \cap \theta_2 = \emptyset} m_1(\theta_1) m_2(\theta_2). \tag{4}$$

To make a final decision, the widely used pignisitc transformation method: $BetP(\cdot)$ was proposed by Smets in [21], which is given as follows: for $\forall \theta \subseteq \Theta$,

$$BetP(\theta) = \sum_{\theta' \subseteq \Theta} m(\theta')(|\theta \cap \theta'|/|\theta'|). \tag{5}$$

And the classical discounting steps are described in details: for $\forall \theta \in 2^{\Theta} \setminus \{\Theta\}$,

$$\begin{cases} m^{\omega}(\theta) = \omega \cdot m(\theta), \\ m^{\omega}(\Theta) = \omega \cdot m(\Theta) + (1-\omega). \end{cases} \tag{6}$$

III. Multi-Criteria based Analysis of Sensor Reliability

We first assume that there exists several BBAs m_i $(i = 1, \cdots, M)$ over the same FoD $\Theta = \{\theta_1, \theta_2, \cdots, \theta_n\}$ (7), which are provided by the independent $A_i,\ i = 1, \cdots, M$ sensors.

$$\begin{array}{c} \\ A_1 \\ A_2 \\ \vdots \\ A_M \end{array} \begin{array}{c} \begin{array}{ccccc} \theta_1 & \theta_2 & \theta_3 & \cdots & \theta_{2^{|\Theta|}} \end{array} \\ \begin{bmatrix} m_1(\theta_1) & m_1(\theta_2) & m_1(\theta_3) & \cdots & m_1(\theta_{2^{|\Theta|}}) \\ m_2(\theta_1) & m_2(\theta_2) & m_2(\theta_3) & \cdots & m_2(\theta_{2^{|\Theta|}}) \\ \vdots & \vdots & \vdots & \ddots & \vdots \\ m_M(\theta_1) & m_M(\theta_2) & m_M(\theta_3) & \cdots & m_M(\theta_{2^{|\Theta|}}) \end{bmatrix} \end{array} \tag{7}$$

where $\theta \in 2^{\Theta}$. According to the traditional strategy of sensor fusion, all these involved sensor readings are combined by Dempster's rule (3) and then the recognition system can acquire the predicted class of the activity according to the final fusion result. However, from the perspective of conflicts between sensors or information redundancy, the reliability of sensors should be evaluated before making the fusion of BBAs. The goal of evaluating sensor reliability is to eliminate or reduce the negative influence of unreliable sensors on the final recognition accuracy. To achieve this goal, the appropriate criterion need to be chosen in advance.

A. Assessment criteria

The involved criteria considered in this work can be divided into two main classes. The first class of criteria relates to the conflict between sensor readings provided by each sensor combination. The second class related to the sensor readings themselves. Combined together, these two criteria are deemed to yield a more efficient and comprehensive assessment of sensors really useful for the recognition system.

1) Conflict using interval distance d_{BI}: The interval distance between evidences between two BBAs m_1 and m_2 expressed in their vector form is given by Han [22]:

$$d_{BI}(m_1, m_2) = \sqrt{Nom \cdot \sum_{ii=1}^{2^n-1} [d^I(BI_1(\theta_{ii}), BI_2(\theta_{ii}))]^2}. \tag{8}$$

Here, Nom is the normalization factor: $Nom = 1/2^{(n-1)}$ and $BI_1(\theta_{ii}) : [Bel_1(\theta_{ii}), Pl_1(\theta_{ii})]$,

$BI_2(\theta_{ii}) : [Bel_2(\theta_{ii}), Pl_2(\theta_{ii})], \quad d^I([a,b],[c,e]) = \sqrt{[\frac{a+b}{2} - \frac{c+e}{2}]^2 + \frac{1}{3}[\frac{b-a}{2} - \frac{e-c}{2}]^2}$.

Thus, we can define the conflict degree (this is criterion Cr_1) between A_i and other involved sensors $A_{i'}$ as follows:

$$Cr_1 = Conflict(A_i) = \frac{1}{M} \cdot \sum_{i'=1}^{M} d_{BI}(m_{A_i}(\cdot), m_{A_{i'}}(\cdot)). \quad (9)$$

2) Imprecision: Within the BF theory, the imperfection of a BBA is mainly determined by strife (Cr_2) [23]. The measure of strife is defined as:

$$Cr_2(m) = St(m) = -\sum_{\theta \in \mathcal{F}(m)} m(\theta) Log_2[\sum_{\theta' \in \mathcal{F}(m)} \frac{|\theta \cap \theta'|}{|\theta|} m(\theta')]. \quad (10)$$

It is important to note that the purpose of using these two aforementioned criteria is to illustrate the effectiveness of our proposed sensor reliability strategy for activity recognition. Of course, more appropriate criteria can be chosen according to the specific problems to be solved in other application contexts such as illness detection.

B. Evaluation of sensor reliability based on BF-TOPSIS

1) Calculating the scoring matrix: Firstly, with A_i, $i = 1, \cdots, M$ sensors, one calculates the reliability of all involved sensors: $\mathbf{A} = \{A_1, A_2, \cdots, A_i, \cdots, A_M\}$ according to each criterion $Cr_j, j = 1, \cdots, N$ and then constructs the following scoring matrix $\mathbf{S}$:

$$\begin{array}{c} \\ Cr_1 \\ Cr_2 \\ \vdots \\ Cr_N \end{array} \begin{array}{c} \begin{array}{ccccc} A_1 & A_2 & A_3 & \cdots & A_M \end{array} \\ \begin{bmatrix} S_1(A_1) & S_1(A_2) & S_1(A_3) & \cdots & S_1(A_M) \\ S_2(A_1) & S_2(A_2) & S_2(A_3) & \cdots & S_2(A_M) \\ \vdots & \vdots & \vdots & \ddots & \vdots \\ S_N(A_1) & S_N(A_2) & S_N(A_3) & \cdots & S_N(A_M) \end{bmatrix} \end{array} \quad (11)$$

And in this paper, $N = 2$: Cr_1 is the conflict measure represented by the distance between two BBAs, and Cr_2 is the imprecision measure. It is noteworthy that the involved criteria here can be adjusted according to the actual needs depending on the chosen application.

2) Construction of BBAs: First, $\mathbf{A} \triangleq \{A_1, A_2, \cdots, A_M\}$ is the special FoD which each element in it represents the independent sensor. And we here use the method presented in [20] to calculate the BBAs:

$$m_j(A_i) \triangleq Bel_j(A_i) \quad (12)$$

$$m_j(\bar{A}_i) \triangleq Bel_j(\bar{A}_i) = 1 - Pl_j(A_i) \quad (13)$$

$$m_j(A_i \cup \bar{A}_i) \triangleq Pl_j(A_i) - Bel_j(A_i). \quad (14)$$

Besides, $Bel_j(A_i)$, $Pl_j(A_i)$ and $Bel_j(\bar{A}_i)$ in (14) are defined as follows:

$$Bel_j(A_i) \triangleq \frac{Sup_j(A_i)}{A^j_{max}} = \frac{\sum_{k \in \{1,\cdots,M\} | S_{jk} \leq S_{ji}} |S_{ji} - S_{jk}|}{max_i Sup_j(A_i)}.$$

$$Bel_j(\bar{A}_i) \triangleq \frac{Inf_j(A_i)}{A^j_{min}} = \frac{-\sum_{k \in \{1,\cdots,M\} | S_{jk} \geq S_{ji}} |S_{ji} - S_{jk}|}{min_i Inf_j(A_i)}.$$

$$Pl_j(A_i) \triangleq 1 - Bel_j(\bar{A}_i).$$

3) BF-TOPSIS Methods:

- Step 1: From the score matrix $\mathbf{S}$, compute BBAs $m_{ij}(A_i)$, $m_{ij}(\bar{A}_i)$ and $m_{ij}(A_i \cup \bar{A}_i)$ using (14);
- Step 2: Compute the belief interval based distance $d_{BI}(m_{ij}, m^{best}_{ij})$ and the distance $d_{BI}(m_{ij}, m^{worst}_{ij})$, where the best ideal BBA is $m^{best}_{ij}(A_i) \triangleq 1$ and the worst ideal BBA is $m^{worst}_{ij}(\bar{A}_i) \triangleq 1$ [22];
- Step 3: Calculate $d_{BI}(m_{ij}, m^{best}_{ij})$ and $d_{BI}(m_{ij}, m^{worst}_{ij})$:

$$d^{best}(A_i) \triangleq \sum_{j=1}^{N} w_j \cdot d_{BI}(m_{ij}, m^{best}_{ij}); \quad (15)$$

$$d^{worst}(A_i) \triangleq \sum_{j=1}^{N} w_j \cdot d_{BI}(m_{ij}, m^{worst}_{ij}). \quad (16)$$

- Step 4: The relative closeness is then defined by

$$Clossness(A_i, A^{best}) \triangleq \frac{d^{worst}(A_i)}{d^{worst}(A_i) + d^{best}(A_i)}. \quad (17)$$

- Step 5: (Weights calculation) The weights of each sensor combination can be calculated $Closeness(A_i, A^{best}) \in [0,1]$ using (18), where a larger $\omega(A_i)$ value means a higher degree of reliability.

$$\omega(A_i) \triangleq \frac{Clossness(A_i, A^{best})}{\sum_{i=1}^{M} Clossness(A_i, A^{best})}. \quad (18)$$

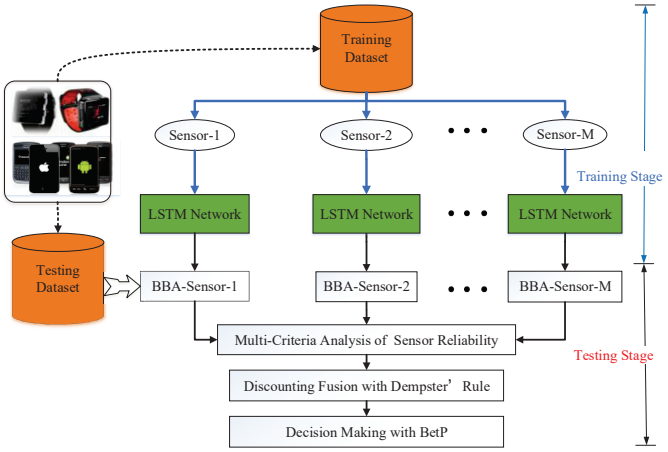

Fig. 1: **The framework of our activity recognition model.**

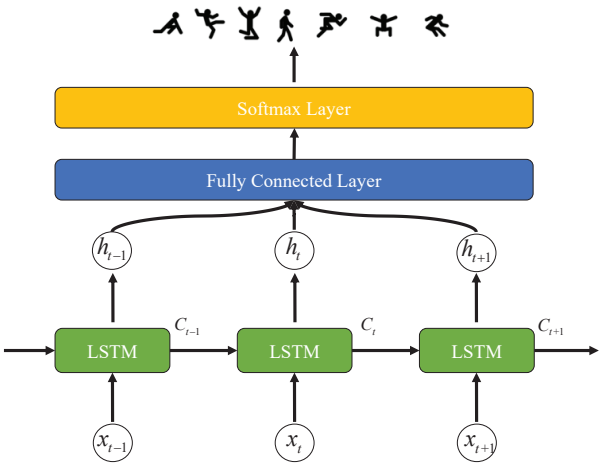

Fig. 2: **Basic LSTM network.**

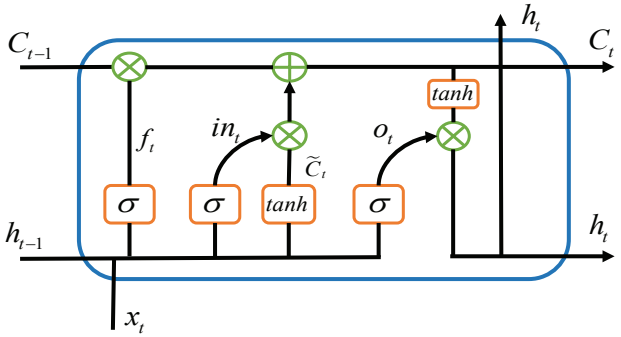

Fig. 3: **Inner structure of LSTM.**

C. The proposed multi-criteria based analysis of sensor reliability

In this paper, the sensor reliability is evaluated by using the conflict and the imprecision. The general process works as follows:

- **Acquisition of sensor readings**. First, the involved sensor readings are constructed which are given as BBAs based on the common FoD;
- **Evaluation of each sensor candidate**. In the second step, we calculate the scoring value of each sensor reading according to the considered criteria and then we construct the scoring matrix;
- **Multi-criteria supports for evaluating sensor reliability**. After the construction of the scoring matrix, the ranking list drawn from the BF-TOPSIS approach and then we can calculate the related weights using (18);

IV. Application to Activity Recognition

In this part, the practical application of activity recognition in BSNs [24–26] is presented. A flow chart of our proposed recognition system based on MCASR is shown in Fig.1.

A. Training stage

As shown in our proposed framework of activity recognition (Fig.1), in the training stage, we use the classical LSTM as the basic classifier to learn the high-level features from raw data collected by sensors. The LSTM was originally proposed by Hochreiter and Schmidhuber in [27]. Untill now, the LSTM has been successfully applied to solve many complex tasks, such as video sequence prediction [28] and natural language processing [29].

Here, we consider an n-class classification problem. That is to say, an instance with its corresponding pattern $\mathbf{x}$ has to be classified among n classes, denoted as $\Theta = \{\theta_1, \theta_2, \cdots, \theta_n\}$. Generally, in our following experiments, the raw data will be first divided into two parts: training dataset and testing dataset. The training data $\mathbf{X} = \{\mathbf{x}_l = \{x_{l1}, x_{l2}, \cdots, x_{lp}\} | l = 1, \cdots, L\}$ is acquired by sensors in BSNs with known classes, where p is the number of attributes and L is the number of instances.

Besides, the structure of the basic LSTM network and the inner structure of the LSTM are given in Fig.2 and Fig.3. As shown in Fig.3, we herein denote the input gate, forget gate, output gate and two memory cell states as $in_t, f_t, o_t, \tilde{C}_t$ and C_t, respectively:

$$in_t = \sigma(W_{in}[h_{t-1}, \mathbf{x}_t] + b_{in}); \tag{19}$$
$$f_t = \sigma(W_f[h_{t-1}, \mathbf{x}_t] + b_f); \tag{20}$$
$$\tilde{C}_t = tanh(W_C[h_{t-1}, \mathbf{x}_t] + b_C); \tag{21}$$
$$C_t = f_t * C_{t-1} + in_t * \tilde{C}_t; \tag{22}$$
$$o_t = \sigma(W_o[h_{t-1}, \mathbf{x}_t] + b_o); \tag{23}$$
$$h_t = o_t * tanh(C_t). \tag{24}$$

where the sigmoid function is as follows:

$$\sigma(x) = \frac{1}{1 + e^{-x}}. \tag{25}$$

Finally, we can obtain the outputs of LSTM Network as follows:

$$\hat{y} = softmax(z) = softmax(W^T h_t + b). \tag{26}$$

where the definition of softmax function is

$$softmax(z_i) = \frac{e^{z_i}}{\sum_{i=1}^{n} e^{z_i}}. \tag{27}$$

B. Testing stage

After the training process of the basic LSTM networks is completed, we can easily recognize the unlabeled data based on our activity recognition strategy. Considering that each trained LSTM corresponds to the specific sensor (we here consider M independent A_i, $i = 1, \cdots, M$ sensors), the output of the LSTM network in (26) is directly used as M BBAs for the wearable sensor:

$$m_1 = \hat{y}_1;$$
$$m_2 = \hat{y}_2;$$
$$\vdots$$
$$m_M = \hat{y}_M.$$

And the proposed MCASR in Section III is applied to assess the reliability degree of each sensor which is denoted as $\omega = \{\omega_1, \omega_2, \cdots, \omega_M\}$. Then, the classical discounting

TABLE I: Three BBAs derived from the outputs of LSTM models.

Belief Mass	θ_1	θ_2	θ_3	θ_4	θ_5	θ_6	θ_7	θ_8	θ_9	θ_{10}	θ_{11}	θ_{12}	Θ
$\mathbf{m}_1$	0.1233	0.1069	0.0382	0.0878	0.0762	0.0415	0.0594	0.0797	0.0399	0.1811	0.1268	0.0394	0
$\mathbf{m}_2$	0.1317	0.0755	0.0273	0.1225	0.0718	0.0792	0.0984	0.0706	0.0782	0.1308	0.0832	0.0308	0
$\mathbf{m}_3$	0.1779	0.0849	0.0329	0.0865	0.0956	0.1178	0.0854	0.1314	0.0616	0.0413	0.0502	0.0345	0

TABLE II: Scoring Matrix for Three Sensor Readings.

$Score(\cdot)$	$\mathbf{m}_1$	$\mathbf{m}_2$	$\mathbf{m}_3$
Conflict Degree (9)	0.0760	0.0610	0.0836
Imprecision (10)	3.4047	3.4657	3.4098

TABLE III: Evidential supports $Sup_j(\mathbf{m}_i)$.

$Sup_j(A_i)$	$\mathbf{m}_1$	$\mathbf{m}_2$	$\mathbf{m}_3$
Conflict (9)	0.0076	0.0376	0
Imprecision (10)	0.0661	0	0.0559

strategy in (6) is used to update all the sensor readings ($m_1^{\omega_1}$, $m_2^{\omega_2}$, $\cdots$, $m_M^{\omega_M}$) and we can combine all these updated SoEs using Dempster's rule (3) which is denoted symbolically by

$$m_{fusion} = Dempster's\ rule(m_1^{\omega_1}, m_2^{\omega_2}, \cdots, m_M^{\omega_M}). \quad (28)$$

Finally, $BetP(\cdot)$ (5) is used to transform m_{fusion} into the Bayesian belief function m_{fusion}^{BetP}:

$$m_{fusion}^{BetP}(\theta) = \sum_{\theta' \subseteq \Theta} m_{fusion}(\theta')(|\theta \cap \theta'|/|\theta'|). \quad (29)$$

and then the final decision of the predicted class of $\mathbf{x}$ can be made as

$$\theta^* = argmax_\theta m_{fusion}^{BetP}(\theta). \quad (30)$$

where θ^* is a singleton of 2^Θ based on the max of belief mass.

In order to show how our proposed fusion method works in the testing stage, here, we give a simple example to illustrate the principle of the discounting fusion discussed in this paper: assuming that there exists a specific testing sample $\mathbf{x}_{testing}$ with unknown label and three LSTM models trained from three different sensors are used to predict the label of $\mathbf{x}_{testing}$. And three corresonding outputs (BBAs: $\mathbf{m}_1, \mathbf{m}_2, \mathbf{m}_3$) of LSTM models are given in Table I. It is worth noting that the scale of FoD in this simple example is consistent with the experimental discussions in Section V: $\Theta = \{\theta_1, \cdots, \theta_{12}\}$ and $2^\Theta = \{\theta_1, \cdots, \theta_{12}, \Theta\}$. In Θ, each singleton represents a kind of the specific activity and Θ in 2^Θ represents the unknown activity. Based on (9) and (10), the scoring matrix related with conflict and imprecision can be calculated and presented in Table II. We can observe that $\mathbf{m}_3$ has the highest conflict degree compared with other sensor readings and $\mathbf{m}_1$ has the lowest degree of imprecision among all considered BBAs.

Then, we can get the positive and negative evidence supports of each sensor ($A_1 : \mathbf{m}_1, A_2 : \mathbf{m}_2, A_3 : \mathbf{m}_3$) based on (14) which are given in Table III and Table IV. After that, the derived inner BBA of each sensor A_i can be also obtained using (14) shown in Table V and Table VI. From the perspective of conflict measure (Table V), $A_2 : \mathbf{m}_2$ obtains the largest supporting degree and on the contrary, $A_1 : \mathbf{m}_1$ can get the hightest supporting degree by using imprecision measure. And then, by using the specific step 3 and step 4 in BF-TOPSIS method, we can get the following distance values, and the relative closeness measures listed in Table VII. We can calculate the weights of all involved sensors based on (18) and then original BBAs ($\mathbf{m}_1, \mathbf{m}_2, \mathbf{m}_3$) are discounted by using the discounting rule (6) and fused with DS rule (3). The related fusion results are given in Table VIII. In the final step, we just use $BetP(\cdot)$ (29) to transform $\mathbf{m}_{fusion}$ into $\mathbf{m}_{fusion}^{BetP}$:

$$\begin{aligned}
&m_{fusion}^{BetP}(\theta_1) = 0.1199; m_{fusion}^{BetP}(\theta_2) = 0.0888;\\
&m_{fusion}^{BetP}(\theta_3) = 0.0522; m_{fusion}^{BetP}(\theta_4) = 0.0923;\\
&m_{fusion}^{BetP}(\theta_5) = 0.0808; m_{fusion}^{BetP}(\theta_6) = 0.0755;\\
&m_{fusion}^{BetP}(\theta_7) = 0.0792; m_{fusion}^{BetP}(\theta_8) = 0.0873;\\
&m_{fusion}^{BetP}(\theta_9) = 0.0661; m_{fusion}^{BetP}(\theta_{10}) = 0.1140;\\
&m_{fusion}^{BetP}(\theta_{11}) = 0.0904; m_{fusion}^{BetP}(\theta_{12}) = 0.0534.
\end{aligned}$$

and we can make the final decision that θ_1 is the predicted class of $\mathbf{x}_{testing}$ based on (30).

TABLE IV: Evidential supports $Inf_j(\mathbf{m}_i)$.

$Inf_j(\mathbf{m}_i)$	$\mathbf{m}_1$	$\mathbf{m}_2$	$\mathbf{m}_3$
Conflict (9)	-0.0150	0	-0.0302
Imprecision (10)	0	-0.1169	-0.0051

TABLE V: BBAs construction of the sensor based on $Conflict$.

Sensor reading	$m_{i1}(A_i)$	$m_{i1}(\bar{A}_i)$	$m_{i1}(A_i \cup \bar{A}_i)$
$A_1 : \mathbf{m}_1$	0.2021	0.4967	0.3012
$A_2 : \mathbf{m}_2$	1.0000	0.0000	0.0000
$A_3 : \mathbf{m}_3$	0.0000	1.0000	0.0000

V. Experimental Results and Discussions

In this part, we show the effectiveness of our proposed activity recognition method based on MCASR. To do these experiments, a well-known activity recognition dataset $mHealth$[1] is chosen from the UCI Machine Learning repository [30]. In addition, all related experiments in this paper are implemented in MATLAB™R2019b environment running on the PC with Intel Core i5-6500 CPU (Window 10).

A. Dataset: mHealth

The raw data in mHealth activity recognition dataset [30] were collected from heterogeneous sensors. These independent sensors were deployed on the subject's chest, right or left arm and right or left ankle. The involved sensor types consist of accelerometer and magnetic, and the whole collected dataset comprises daily activity recordings for ten volunteers

[1] http://archive.ics.uci.edu/ml/datasets/MHEALTH+Dataset.

TABLE VI: BBAs construction of the sensor based on $Imprecision$.

Sensor reading	$m_{i2}(A_i)$	$m_{i2}(\bar{A}_i)$	$m_{i2}(A_i \cup \bar{A}_i)$
$A_1 : \mathbf{m}_1$	1.0000	0.0000	0.0000
$A_2 : \mathbf{m}_2$	0.0000	1.0000	0.0000
$A_3 : \mathbf{m}_3$	0.8457	0.0436	0.1107

of diverse profile while performs 12 physical activities. These activities are standing still, sitting and relaxing, lying down, walking, climbing stairs, waist bends forward, frontal elevation of arms, knees bending, cycling, jogging, running, jump front and back. For the convenience of further discussions, we just labelled such twelve activities as V1-V12, respectively. The modalities from the sensors were recorded at a sampling rate of 50 Hz and this dataset has 1,215,745 instances in total and has reasonably well balanced classes. In this paper, we here only consider those raw data collected from Accelerometers located on Chest (AC), Left Ankle (ALA) and Right Lower Arm (ARLA). Besides, a 10-fold cross-validation technique is chosen for mHealth data to generate the training instances (80%) and the testing instances (20%).

B. Measures of performances

As measures of performances of our activity recognition system, we consider the classical Accuracy defined by

$$Accuracy = \frac{1}{n}\sum_{k=1}^{n}\frac{\mathrm{TP}_k + \mathrm{TN}_k}{\mathrm{TP}_k + \mathrm{TN}_k + \mathrm{FP}_k + \mathrm{FN}_k}. \qquad (31)$$

where TP_k, FP_k and FN_k are respectively the number of correctly recognized class examples (true positives: TP), examples that were either incorrectly assigned to the class (false positives: FP) and not recognized as class examples (false negatives: FN).

C. Experimental setup

In this paper, we have made the comparisons between our proposed method and start-of-the-art methods. These classical approaches include: (1) Support Vector Machine (SVM): the input vectors derived from the segmented raw signals, are used as the input of SVM model. Similar to HMM, the SVM models are trained with the classical One-vs-all strategy and the number of SVM models is consistent with the number of activity classes; (2) Hidden Conditional Random Fields (HCRF): each HCRF model is trained by using three hidden states and we select the highest scoring model among all one-vs-all HCRF models; (3) Convolutional Neural Networks with 2D kernel (2D CNN): here, we consider CNN using 2D convolution kernel and 2D pooling kernel.

In our proposed method (Fig.1), raw data collected from three sensors (AC, ALA and ARLA) are used to train three basic LSTM network. The default parameters of LSTM network are: the number of features for the input layer is 3 (axis-x,y,z); the number of hidden units is 70; the total epoch is 50 with an early stopping criteria. For the convenience of representation and comparisons in the following sections, we just use abbreviations to denote basic LSTM network and our proposed model: AC, ALA and ARLA means that LSTM network is trained by raw data collected from accelerator located on chest, left ankle and right lower arm, respectively. And fused LSTM network refers to our proposed model which aims to combine all basic LSTM (AC, ALA, ARLA) using MCASR. Besides, in our proposed MCASR, the important parameter values are fixed: $M = 3$ which represents that in this specific application, sensor readings collected from three sensors (AC, ALA, ARLA) are considered for fusion; $n = 12$ means that there are twelve predefined activities which need to be classified; $N = 2$ is the number of assessment criteria which are defined in (9) and (10); In this application, considering that there are nearly twelve activities to be classified, we simplify the power set space and only consider the incomplete power set space: $2^{\Theta}_{refined} = \{\theta_1, \cdots, \theta_{12}, \Theta\}$.

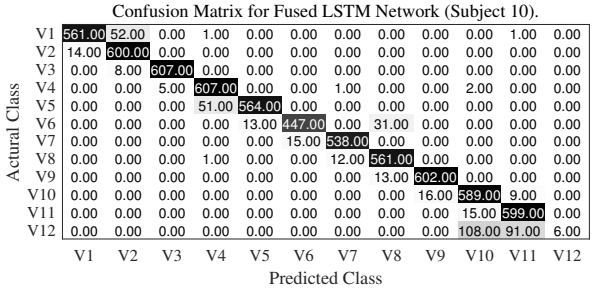

Fig. 4: **Confusion matrix of subject 10 in UCI mHealth dataset based on our proposed fused LSTM.**

D. Experimental results

1) Main performance of the fused LSTM model for each subject: For subject 1 in mHealth, our proposed fused LSTM network achieves the mean prediction performance of 0.9433. Similarly, for subject 2-10, it achieves 0.8663, 0.9193, 0.8749, 0.8566, 0.9046, 0.9049, 0.8826, 0.9335, 0.8613. In order to show the accuracy of each activity, we also give the specific confusion matrix of subject 10 in Fig.4. By looking at the confusion matrix of our fused LSTM network in Fig.4, we see that the corresponding accuracy of twelve activities based on our fused model is significantly different: the activity with the highest recognition accuracy (0.9870) is V3 (lying down) and the type of activity with the lowest recognition accuracy is V12 (jump front and back); for other defined activities: V1-V2, V4-V11, our fused model could give relative good performance and the average accuracies of these ten remaining activities are 91.22%, 97.72%, 98.70%, 91.71%, 91.04%, 97.29%, 97.76%, 97.89%, 97.52%, 97.56%. However, for all subjects, our fused LSTM model has the lowest performance in recognizing V12 (jump front and back). This class is more misclassified as jogging (V10) or running (V11) which might be related to the pace that each individual takes to perform these activities. In order to observe the spatial relationship between these three complex activities, we just draw the corresponding original data in Fig.5. It is obvious that although the accelerators are deployed on different locations of bodies, the overlap of these three activities is very high, which directly affects the classification accuracy of our proposed model. This also further

TABLE VII: Distance and relative closeness measures.

Sensor	$d_{BI}^{E}(m_{ij}, m_{ij}^{best})$	$d_{BI}^{E}(m_{ij}, m_{ij}^{worst})$	$Clossness(A_i, A^{best})$	$\omega(A_i)$
$\mathbf{m}_1$	0.9870	2.0346	0.6734	0.4167
$\mathbf{m}_2$	1.4143	1.4142	0.5000	0.3093
$\mathbf{m}_3$	1.6091	1.2815	0.4433	0.2740

TABLE VIII: Discounted Three BBAs and Final Fusion BBA.

Belief Mass	θ_1	θ_2	θ_3	θ_4	θ_5	θ_6	θ_7	θ_8	θ_9	θ_{10}	θ_{11}	θ_{12}	Θ
$\mathbf{m}_1^{\omega_1}$	0.1233	0.1069	0.0382	0.0878	0.0762	0.0415	0.0594	0.0797	0.0399	0.1811	0.1268	0.0394	0
$\mathbf{m}_2^{\omega_2}$	0.1317	0.0755	0.0273	0.1225	0.0718	0.0792	0.0984	0.0706	0.0782	0.1308	0.0832	0.0308	0
$\mathbf{m}_3^{\omega_3}$	0.1779	0.0849	0.0329	0.0865	0.0956	0.1178	0.0854	0.1314	0.0616	0.0413	0.0502	0.0345	0
$\mathbf{m}_{fusion}$	0.0880	0.0569	0.0202	0.0604	0.0489	0.0435	0.0473	0.0553	0.0342	0.0821	0.0585	0.0214	0.3833

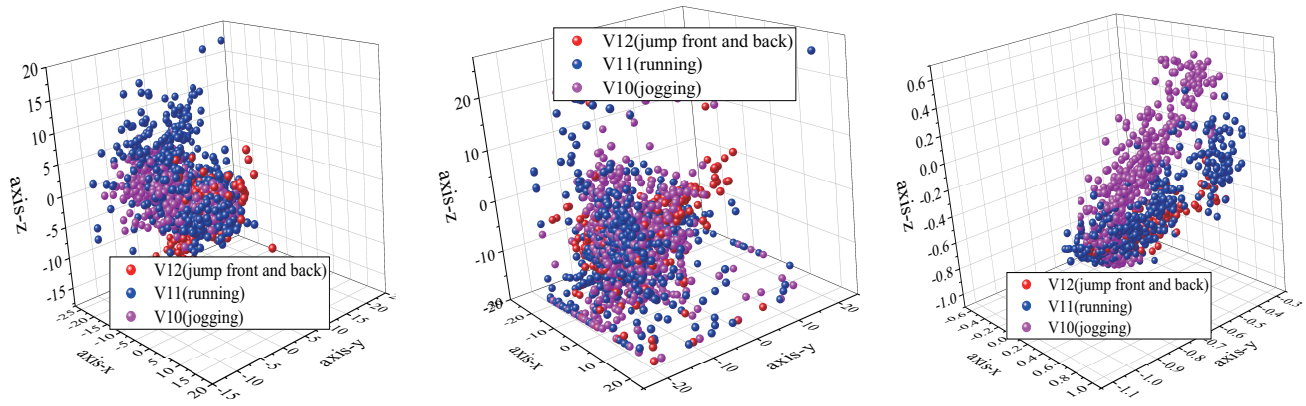

(a) Raw data collected from accelerator deployed on the chest

(b) Raw data collected from accelerator deployed on left ankle

(c) Raw data collected from accelerator deployed on the right lower arm

Fig. 5: **Raw data corresponding to three activities (V10, V11, V12) which are collected from three accelerators located on chest, left ankle and right lower arm, respectively.**

illustrates that more wearable sensors need to be deployed on body to sense such complex activities, which means that a single accelerator sensor deployed on three locations is not enough.

TABLE IX: Comparison of the Proposed Fused LSTM network with State-of-The-Art Methods on the UCI mHealth dataset.

Method	Precision	Time (s) (train/test)
SVM	65.40%	76.5/0.4
HCRF	68.60%	124/2.0
2D CNN [31]	89.14%	634.1/0.3
Posterior-Adapted Fusion [32]	88.59%	173/13
Automated Feature Classifier [33]	76.44%	130.4/1.2
DSmT-Based Classifier [25]	88.46%	94.3/0.2
Multiscale DCNN Ensemble [34]	83.99%	634.1/0.6
Autonomous Encoders [35]	82.00%	209.9/31
Our Proposed Fused LSTM	**91.12%**	**449.9/0.3**

2) Compared to State-of-the-Art approaches: In order to compare the proposed fused LSTM network with other traditional methods, several baseline approaches are implemented herein which were shown in Table IX. We can obviously see that the average accuracy of fused LSTM is the highest. By comparisons, those models (SVM, HCRF, BDT, DSmT-based KDE) trained by hand-crafted features had relatively lower accuracy. Since 2D-CNN can extract deep features using deep neural network, it performed better than other traditional methods. However, such single model didn't consider the important issue of sensor reliability and directly assumes that all involved sensors have the same weights. Based on this premise, all sensor readings are used to train their models which in some degree affects the performance of activity recognition. In terms of training computational cost, the listed three models using deep learning framework: 2D CNN, Mulis-cale DCNN Ensemble and our proposed Fused LSTM required more training time than the other traditional methods. At the same time, the classical SVM and our previous model DSmT-Based Classifier have the lowest training time in Table IX. This mainly because that these two methods used the traditional manual feature selection and training strategies without deep learning architecture. Therefore, the training time of these two models is lower than other models, which is reasonable. In terms of the testing computational cost, our proposed fused LSTM is highly competitive which has the average testing time similar to SVM, 2D CNN, DSmT-Based Classifier. However, the training time of the proposed fused LSTM is superior than others and this is mainly because that there are several basic LSTM networks which are required to be trained in our proposed ensemble recognition framework Fig.1.

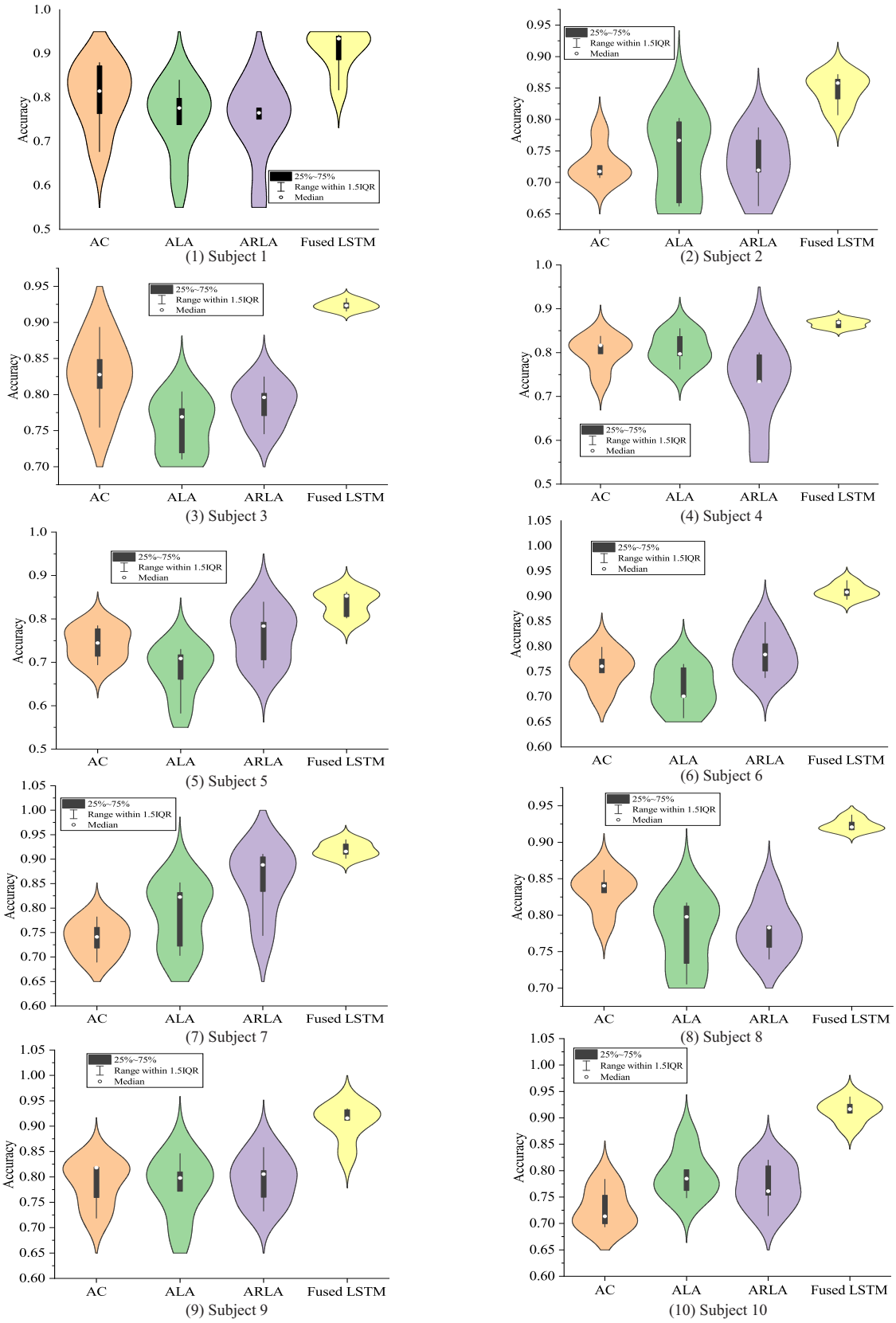

Fig. 6: **Violin box-plot showing the dispersion of accuracy of the basis LSTM and fused LSTM (IQR: Inter Quartile Range).**

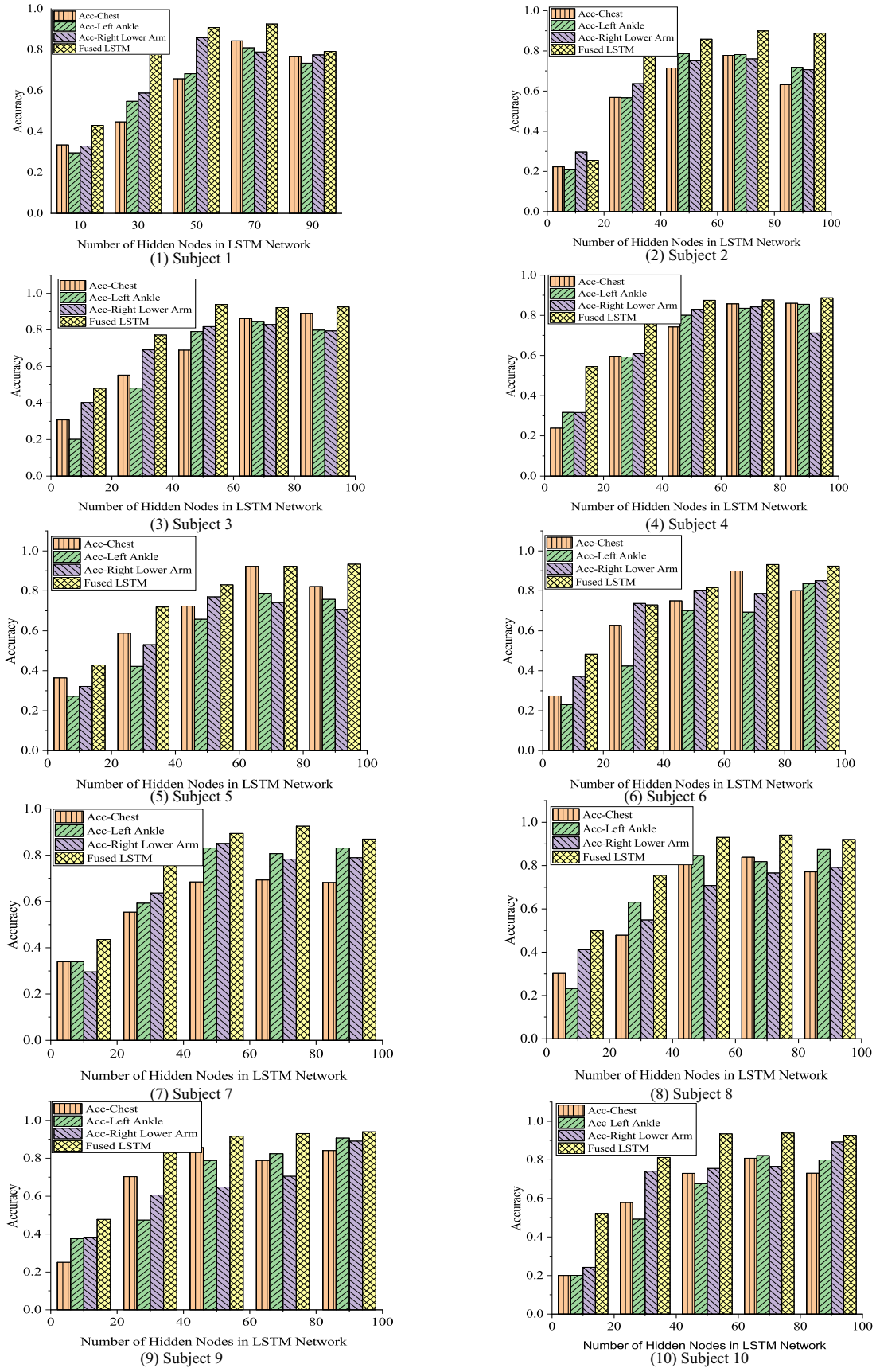

Fig. 7: **The impacts of the number of hideen nodes for the performance of LSTM network.**

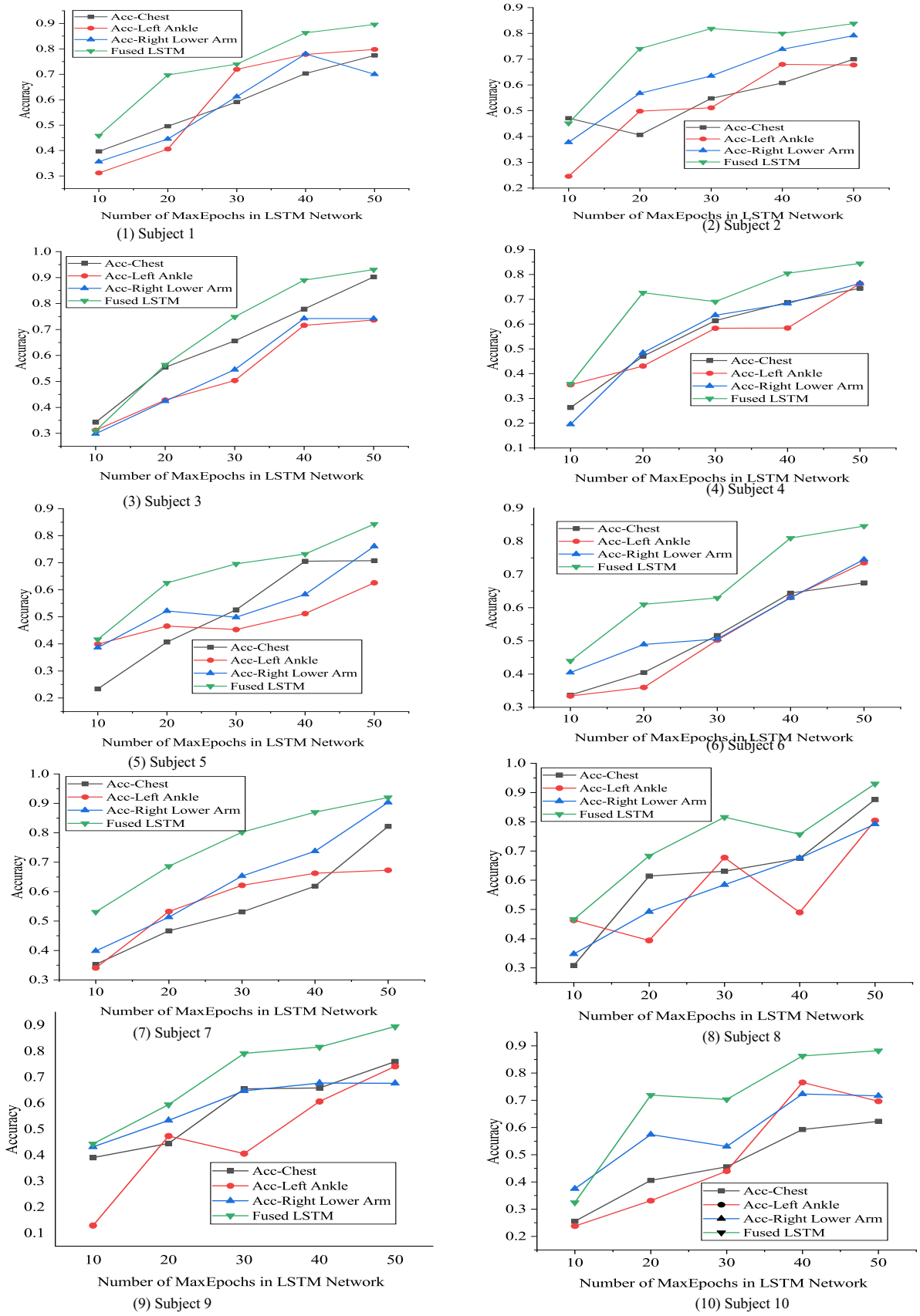

Fig. 8: **The impacts of the number of MaxEpochs for the performance of LSTM network.**

As shown in the framework of our proposed model in Fig.1, we essentially integrates multiple basic LSTMs into the fused model. Thus, we further compare the performances of basic LSTMs and fused LSTM, which was shown in Fig.6. Considering the mHealth dataset, we can observe a plot containing 10 violin box-plots representing the variation/dispersion of the accuracy per model in Fig.6. In this figure, we notice that fused LSTM network (yellow) has less dispersion in accuracy that other basic LSTMs for all ten individuals. And the median accuracy (white circle) of fused LSTM is obviously better than all mentioned basic LSTMs. This shows, once again, the superiority and effectiveness of our proposed fused LSTM with MCASR.

E. Impacts of hidden nodes and MaxEpochs in LSTM

1) Number of hidden nodes in LSTM network: For the LSTM network, the number of hidden layer nodes in the network is directly related to the performance of the recognition model. Here, we focus our discussions on the impact of this key parameter on the recognition accuracy for three basic LSTMs trained by raw data collected from AC, ALA, ARLA, and the proposed fused LSTM network with MCASR using the mHealth dataset. We can clearly find in Fig.7 that the accuracies of all basic LSTM models and also fused LSTM network increases with more hidden nodes (from 10 to 90). However, when the number of hidden nodes is greater than a certain number, the accuracies become stable. Thus, the default value (70) of epochs for our proposed fused LSTM network is proper. Our proposed fused LSTM network with MCASR achieves the best performance by taking the advantages of MCASR and ensemble framework.

2) Number of MaxEpochs in LSTM network: In addition to the number of hidden nodes, another important hyperparameter is the number of epochs in the training process of LSTM network. Here, we further explore the impact of this parameter on recognition accuracy for three basic LSTMs trained by raw data collected from AC, ALA, ARLA, and the proposed fused LSTM network with MCASR using the mHealth dataset. The recognition accuracies for all the approaches with the number of epochs from 10 to 50 are shown in Fig.8. We can find that the accuracies of all the approaches increase with more epochs. Similar to the previous experimental results, our proposed fused LSTM network also performs better than basic LSTM models, which indicates the merits of MCASR and our framework of activity recognition. As we all know that the use of higher numbers of epochs will lead to longer training time, thus, the selection of this parameter is a tradeoff between training time and recognition accuracy. Taking training time into consideration, the default value (50) of epochs for our proposed fused LSTM network is proper.

VI. Conclusion

In this paper, we have proposed a novel analysis of sensor reliability coupled with multi-criteria support. Besides, a new framework for activity recognition based on the proposed MCASR has also been described and tested. At first, we use BF-TOPSIS to assess the reliability of sensors according to multi-criteria. In this paper, two common used criteria are conflict between sensor readings and imprecision degree of sensor readings. Then, in our application section, we also propose a novel ensemble framework for activity recognition using basic LSTM network with MCASR. Finally, we have verified the validity of the proposed method by classifying twelve daily activities in UCI mHealth dataset. The simulation results show that our proposed fused LSTM network can give the highest accuracy compared with state-of-art approaches. In our future works, more complex activity recognition problems will be also considered with different decision-making strategies in BF theory. Besides, in order to realize the detailed analysis of misclassification, we will further study and discuss the interpretability of our proposed activity recognition model [36, 37].

Acknowledgment

The authors thank the reviewers and editors for giving valuable comments, which are very helpful for improving this manuscript.

References

[1] R. Gravina, P. Alinia, H. Ghasemzadeh, and G. Fortino, "Multi-sensor fusion in body sensor betworks: state-of-the-art and research challenges," *Information Fusion*, vol. 35, pp. 68–80, 2017.

[2] S. Nekooei and G. Chen, "Cooperative coevolution design of multilevel fuzzy logic controllers for media access control in wireless body area networks," *IEEE Transactions on Emerging Topics in Computational Intelligence*, vol. 4, no. 3, pp. 336–350, 2020.

[3] C. Michaelides and F.-N. Pavlidou, "Uplink NOMA in body area networks with simple node pairing strategies," *IEEE Sensors Journal*, vol. 20, no. 16, pp. 9596–9603, 2020.

[4] S. M. Mathews, C. Kambhamettu, and K. E. Barner, "Centralized class specific dictionary learning for wearable sensors based physical activity recognition," in *2017 51st Annual Conference on Information Sciences and Systems (CISS)*. IEEE, 2017, pp. 1–6.

[5] ——, "Maximum correntropy based dictionary learning framework for physical activity recognition using wearable sensors," in *International Symposium on Visual Computing*. Springer, 2016, pp. 123–132.

[6] A. B. Sargano, X. Wang, P. Angelov, and Z. Habib, "Human action recognition using transfer learning with deep representations," in *2017 International joint conference on neural networks (IJCNN)*. IEEE, 2017, pp. 463–469.

[7] S. M. Mathews, "Dictionary and deep learning algorithms with applications to remote health monitoring systems," Ph.D. dissertation, University of Delaware, 2017.

[8] A. Wang, S. Zhao, C. Zheng, H. Chen, L. Liu, and G. Chen, "Hierhar: sensor-based data-driven hierarchical human activity recognition," *IEEE Sensors Journal*, vol. 21, no. 3, pp. 3353–3365, 2021.

[9] K. Viard, M. P. Fanti, G. Faraut, and J. J. Lesage, "Human activity discovery and recognition using probabilistic finite-state automata," *IEEE Transactions on Automation Science and Engineering*, vol. 17, no. 4, pp. 2085–2096, 2020.

[10] G. Nimisha, P. Rourab, M. Satyabrata, M. Krishanu, and S. Sayantan, "Fault matters: sensor data fusion for detection of faults using Dempster–Shafer theory of evidence in IoT-based applications," *Expert Systems with Applications*, vol. 162, pp. 1138–1147, 2020.

[11] Z. Liu, Y. Liu, J. Dezert, and F. Cuzzolin, "Evidence combination based on credal belief redistribution for pattern classification," *IEEE Transactions on Fuzzy Systems*, vol. 28, no. 4, pp. 618–631, 2020.

[12] A. Rubio-Solis, G. Panoutsos, C. Beltran-Perez, and U. Martinez-Hernandez, "A multilayer interval type-2 fuzzy extreme learning machine for the recognition of walking activities and gait events using wearable sensors," *Neurocomputing*, vol. 389, pp. 42–55, 2020.

[13] H. Ayadi, A. Zouinkhi, T. Val, A. van den Bossche, and M. N. Abdelkrim, "Network lifetime management in wireless sensor networks," *IEEE Sensors Journal*, vol. 18, no. 15, pp. 6438–6445, 2018.

[14] A. Jamal, V. P. Namboodiri, D. Deodhare, and K. Venkatesh, "Deep domain adaptation in action space." in *29th British Machine Vision Conference*, vol. 2, 2018, p. 264.

[15] H. Rezaie and M. Ghassemian, "An adaptive algorithm to improve energy efficiency in wearable activity recognition systems," *IEEE Sensors Journal*, vol. 17, no. 16, pp. 5315–5323, 2017.
[16] M. M. Moallem, A. Aghagolzadeh, and R. Ghazalian, "Wireless visual sensor networks energy optimization based on new entropy model," *IEEE Sensors Journal*, vol. 20, no. 2, pp. 1321–1331, 2020.
[17] M. Monemian, M. Mahdavi, and M. J. Omidi, "Optimum sensor selection based on energy constraints in cooperative spectrum sensing for cognitive radio sensor networks," *IEEE Sensors Journal*, vol. 16, no. 6, pp. 1829–1841, 2016.
[18] X. Huang, Y. Wu, F. Ke, K. Liu, and Y. Ding, "An energy-efficient and reliable scheduling strategy for dynamic WBANs with channel periodicity exploitation," *IEEE Sensors Journal*, vol. 20, no. 5, pp. 2812–2824, 2020.
[19] O. Khutsoane, B. Isong, N. Gasela, and A. M. Abu-Mahfouz, "Watergrid-sense: a lora-based sensor node for industrial IoT Applications," *IEEE Sensors Journal*, vol. 20, no. 5, pp. 2722–2729, 2020.
[20] J. Dezert, D. Han, and H. Yin, "A new belief function based approach for multi-criteria decision-making support," in *Information Fusion (FUSION), 2016 19th International Conference on*. IEEE, 2016, pp. 782–789.
[21] G. Shafer, *A mathematical theory of evidence*. Princeton university press, 1976, vol. 42.
[22] D. Han, J. Dezert, and Y. Yang, "Belief interval-based distance measures in the theory of Belief Functions," *IEEE Transactions on Systems Man and Cybernetics Systems*, vol. 48, no. 6, pp. 833–850, 2018.
[23] Y. Dong, X. Li, J. Dezert, and S. S. Ge, "A novel multi-criteria discounting combination approach for multi-sensor fusion," *IEEE Sensors Journal*, vol. 19, no. 20, pp. 9411–9421, 2019.
[24] Z. Chen, C. Jiang, and L. Xie, "A novel ensemble ELM for human activity recognition using smartphone sensors," *IEEE Transactions on Industrial Informatics*, vol. 15, no. 5, pp. 2691–2699, 2019.
[25] Y. Dong, X. Li, J. Dezert, M. O. Khyam, M. Noor-A-Rahim, and S. S. Ge, "Dezert-Smarandache theory-based fusion for human activity recognition in body sensor networks," *IEEE Transactions on Industrial Informatics*, vol. 16, no. 11, pp. 7138–7149, 2020.
[26] N. Golestani and M. Moghaddam, "Human activity recognition using magnetic induction-based motion signals and deep recurrent neural networks," *Nature Communications*, vol. 11, no. 1, pp. 183–193, 2020.
[27] S. Hochreiter and J. Schmidhuber, "Long Short-Term Memory," *Neural Computation*, vol. 9, no. 8, pp. 1735–1780, 1997.
[28] R. Villegas, J. Yang, S. Hong, X. Lin, and H. Lee, "Decomposing motion and content for natural video sequence prediction," *arXiv preprint arXiv:1706.08033*, 2017.
[29] Q. Zhu, Z. Chen, and Y. C. Soh, "A novel semisupervised deep learning method for human activity recognition," *IEEE Transactions on Industrial Informatics*, vol. 15, no. 7, pp. 3821–3830, 2019.
[30] O. Banos, R. Garcia, J. A. Holgado-Terriza, M. Damas, H. Pomares, I. Rojas, A. Saez, and C. Villalonga, "mhealthdroid: a novel framework for agile development of mobile health applications," in *International Workshop on Ambient Assisted Living*, 2014, pp. 91–98, http://archive.ics.uci.edu/ml/datasets/mhealth+dataset.
[31] H. Sojeong and C. Seungjin, "Convolutional neural networks for human activity recognition using multiple accelerometer and gyroscope sensors," in *2016 International Joint Conference on Neural Networks (IJCNN)*, 2016, pp. 381–388.
[32] A. K. Chowdhury, D. Tjondronegoro, V. Chandran, and S. G. Trost, "Physical activity recognition using posterior-adapted class-based fusion of multiaccelerometer data," *IEEE Journal of Biomedical and Health Informatics*, vol. 22, no. 3, pp. 678–685, 2018.
[33] E. Zdravevski, P. Lameski, V. Trajkovik, A. Kulakov, I. Chorbev, R. Goleva, N. Pombo, and N. Garcia, "Improving activity recognition accuracy in ambient-assisted living systems by automated feature engineering," *IEEE ACCESS*, vol. 5, pp. 5262–5280, 2017.
[34] S. Jessica, B. Jesimon, C. Carlos, C. Guilherme, and S. William, Robson, "Human activity recognition based on smartphone and wearable sensors using multiscale DCNN ensemble," *Neurocomputing*, vol. -, pp. –, 2021.
[35] G. Kemilly, R. Cláudio, P. Mannes, and C. Tiago, "An ensemble of autonomous auto-encoders for human activity recognition," *Neurocomputing*, vol. 439, pp. 271–280, 2021.
[36] S. M. Mathews, "Explainable artificial intelligence applications in nlp, biomedical, and malware classification: A literature review," in *Intelligent Computing*, K. Arai, R. Bhatia, and S. Kapoor, Eds., 2019, pp. 1269–1292.
[37] R. R. Selvaraju, M. Cogswell, A. Das, R. Vedantam, D. Parikh, and D. Batra, "Grad-cam: Visual explanations from deep networks via gradient-based localization," in *Proceedings of the IEEE international conference on computer vision*, 2017, pp. 618–626.

Yilin Dong was born in Yancheng, China, in 1990. He received the Ph.D. degree in Control Science and Engineering from the School of Automation, Southeast University, Nanjing, China, in 2020. Afterwards, he joined College of Computer Science and Engineering, Shanghai Maritime University, Shanghai, China. His research interests include belief function theory, information fusion, and pattern recognition.

Xinde Li (M'09-SM'16) earned his Ph.D. in Control Theory and Control Engineering, from Department of Control Science and Engineering, Huazhong University of Science and Technology (HUST),Wuhan, China, in 2007. Afterwards, he joined School of Automation, Southeast University, Nanjing, China, where he is currently a Professor and Ph.D. Supervisor. His research interests include information fusion, object recognition, computer vision, intelligent robot, and human-robot interaction.

Jean Dezert was born in L'Hay les Roses, France, in 1962. He received the Ph.D. degree from the University Paris XI, Orsay, France, in 1990. Since 1993, he has been a Senior Research Scientist with the Information Modeling and Processing Department, ONERA, Palaiseau, France. His current research interests focus on belief function theory, particularly for DSmT, which he has developed with Prof. Smarandache.

Rigui Zhou received his Ph.D. degree in the Department of Computer Science and Technology of Nanjing University of Aeronautics and Astronauts (November, 2007), China. From 2008 to 2010, as a Post Doctoral fellow in the Tsinghua University, China. Currently he is a Professor of College of Information Engineering, Shanghai Maritime University, China. His research interests include quantum image processing, quantum reversible logic and quantum genetic algorithm, et al.

Changming Zhu received the Ph.D. degree in computer science from the East China University of Science and Technology, Shanghai, China, in 2015. He is currently an Associate Professor with the College of Computer Science and Engineering, Shanghai Maritime University, Shanghai. His current research interests include pattern recognition and machine learning.

Shuzhi Sam Ge (S'90–M'92-SM'99–F'06) received the B.Sc. degree from the Beijing University of Aeronautics and Astronautics, Beijing, China, in 1986, and the Ph.D. degree from Imperial College of Science, Technology and Medicine, University of London, London, U.K., in 1993. He is currently the Founding Director of the Robotics Institute and the Institute of Intelligent Systems and Information Technology, University of Electronic Science and Technology of China, Chengdu, China. He is also the Founding Director of the Social Robotics Laboratory, Interactive Digital Media Institute, National University of Singapore, Singapore, where he is a Professor with the Department of Electrical and Computer Engineering. He is the Editor-in-Chief of the International Journal of Social Robotics. He has served as an associate editor for a number of flagship journals. He has also served as the Vice-President of Technical Activities from 2009 to 2010, Membership Activities from 2011 to 2012, and the IEEE Control Systems Society.